J. Math. Biol. 50, 189–207 (2005)
Digital Object Identifier (DOI):
10.1007/s00285-004-0286-2

Mathematical Biology

Francis Filbet · Philippe Laurençot · Benoît Perthame

Derivation of hyperbolic models for chemosensitive movement

Received: 4 November 2003 / Revised version: 14 June 2004 /
Published online: 7 October 2004

Abstract. A Chapman-Enskog expansion is used to derive hyperbolic models for chemosensitive movements as a hydrodynamic limit of a velocity-jump process. On the one hand, it connects parabolic and hyperbolic chemotaxis models since the former arise as diffusion limits of a similar velocity-jump process. On the other hand, this approach provides a unified framework which includes previous models obtained by *ad hoc* methods or methods of moments. Numerical simulations are also performed and are motivated by recent experiments with human endothelial cells on matrigel. Their movements lead to the formation of networks that are interpreted as the beginning of a vasculature. These structures cannot be explained by parabolic models but are recovered by numerical experiments on hyperbolic models. Our kinetic model suggests that some kind of local interactions might be enough to explain them.

Contents

F. Filbet: Mathématiques et Applications, Physique Mathématique d'Orléans, CNRS UMR 6628, Université d'Orléans, B.P. 6759, 45067 Orléans cedex 2, France.
e-mail: filbet@labomath.univ-orleans.fr

P. Laurençot: Mathématiques pour l'Industrie et la Physique, CNRS UMR 5640, Université Paul Sabatier – Toulouse 3, 118 route de Narbonne, 31062 Toulouse cedex 4, France.
e-mail: laurenco@mip.ups-tlse.fr

B. Perthame: Département de Mathématiques Appliquées, CNRS UMR 8553, Ecole Normale Supérieure, 45, rue d'Ulm, 75230 Paris cedex 05, France.
e-mail: benoit.perthame@ens.fr

1. Introduction

Chemotaxis is a process by which cells change their state of movement reacting to the presence of a chemical substance, approaching chemically favorable environments and avoiding unfavorable ones. In the simple situation where we only consider cells and a chemical substance (the chemo-attractant), a model for the space and time evolution of the density $n = n(t, x)$ of cells and the chemical concentration $S = S(t, x)$ at time t and position $x \in \Omega \subset \mathbb{R}^d$ has been introduced by Patlak [28] and Keller & Segel [17] and reads

$$\frac{\partial n}{\partial t} - \operatorname{div}(D\nabla n - \chi\, n\nabla S) = 0, \tag{1}$$

$$\frac{\partial S}{\partial t} - D_S\, \Delta S = g(n, S). \tag{2}$$

However, this approach is not always sufficiently precise to describe the evolution of bacteria movements. Indeed, experiments show that bacteria like *Escherichia Coli* move along straight lines, suddenly stop to choose a new direction and then continue moving in a new direction. This phenomenon, called run and tumble, can

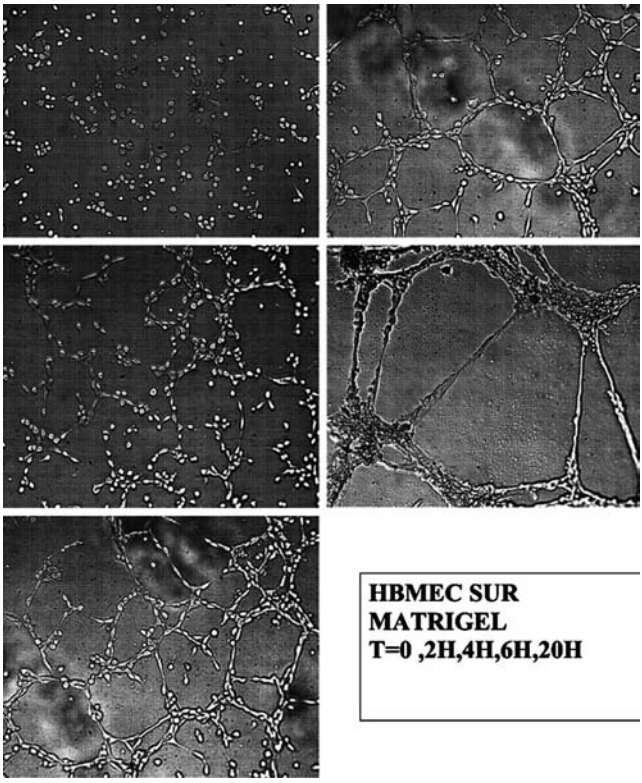

Fig. 1. Formation of network of endothelial cells (courtesy of *Dr.* M. Mirshahi).

be modeled by a stochastic process called the velocity-jump process, and has been introduced by Alt [1] and further developed in [11,32]. A kinetic transport model to describe this velocity jump process reads [27]

$$\frac{\partial f}{\partial t} + v \cdot \nabla_x f = \mathcal{T}(S, f), \tag{3}$$

where $f(t, x, v)$ denotes the density of cells, depending on time t, position x and velocity v and $\mathcal{T}$ is an operator, which models the change of direction of cells. In fact, parabolic chemotaxis equations such as the Patlak-Keller-Segel (PKS) model (1)–(2) have been obtained as the diffusion limit of the transport equation (3), thus allowing to determine the motility D and the chemotactic sensitivity χ [11,26]. A mathematical convergence proof has been subsequently supplied in [2], while we refer to [2,16] for the existence of solutions to (3). More precisely, the diffusion limit may be seen as the limit of (3) as ε goes to zero after the rescaling $t \to \varepsilon^2 t, \quad x \to \varepsilon x$, which shows that the PKS system (1)–(2) corresponds to a long time asymptotics of the transport model. A more recent tendency has been to use hyperbolic equations to describe intermediate regimes at the macroscopic level rather than parabolic equations like (1)–(2), see for instance [4,5,31]. Our purpose is to give several ways toward such modeling and especially to assert hyperbolic chemotaxis models developed either by *ad hoc* methods [31,8] or by a moments closure method [12,13] starting from (3). In this paper, we will show that hyperbolic chemotaxis models may also be derived as a fluid limit of the transport equation (3), but with a different scaling, the hydrodynamic scaling $t \to \varepsilon t, \quad x \to \varepsilon x$. The approach used relies on a Chapman-Enskog (or Hilbert) expansion and allows us to recover the previously mentioned models.

Let us recall recent experiments with human endothelial cells on matrigel. Their movements lead to the formation of networks that are interpreted as the beginning of a vasculature (see Fig. 2 or [31,8]). This phenomenon is important since it is responsible of angiogenesis, a major factor for the growth of tumors [3,19]. These structures cannot be explained by the above parabolic models which generically lead to pointwise blow-up, but are recovered by numerical experiments on hyperbolic models. Our kinetic model suggests that local interactions between cells might be part of the mechanism for these network formations and not only the long range interactions throught a diffused chemoattractant.

The outline of this paper is as follows. In section 2, we give general assumptions on the kinetic transport model (turning operator) and use a formal Chapman-Enskog expansion to derive different hyperbolic systems which depend on the structure of the turning operator $\mathcal{T}$. We first study linear operators with respect to f and point out some of their features. We then use this approach to derive nonlinear hyperbolic models already proposed by Gamba *et al.* [31] to describe the first stages of blood vessels formation. Finally, in section 3 we perform some numerical computations of nonlinear hyperbolic models of chemotaxis, using a second order Lax-Friedrich scheme. On the one hand, we compare the transient behaviour of the parabolic model (PKS system) and hyperbolic models. On the other hand, we observe the formation of networks in hyperbolic models as in the above mentioned experiments.

2. Derivation of hyperbolic systems

2.1. The kinetic framework

We scale the time and space variables $t \to \varepsilon t$ and $x \to \varepsilon x$ in (3) and thus obtain the following transport equation for the distribution function $f = f(t, x, v)$

$$\frac{\partial f}{\partial t} + v \cdot \nabla_x f = \frac{1}{\varepsilon} \mathcal{T}(S, f), \tag{4}$$

where the position $x \in \Omega \subset \mathbb{R}^d$ and the velocity $v \in V \subset \mathbb{R}^d$. Here again, the concentration of the chemo-attractant $S(t, x)$ is a solution to (2), where the density of cells n is given by

$$n(t, x) = \int_V f(t, x, v) dv.$$

As in [11,26], we assume herein that the turning operator is of the form

$$\mathcal{T}(S, f) = \mathcal{T}_0(f) + \varepsilon \mathcal{T}_1(S, f), \tag{5}$$

where $\mathcal{T}_0$ represents the dominant part of the turning kernel modeling the tumble process in the absence of chemical substance and $\mathcal{T}_1$ is the perturbation due to chemical cues. The parameter ε is a time scale which here refers to the turning frequency. The purpose of this paper is to understand the asymptotics of (4) as ε goes to zero.

We first mention some assumptions on the turning operators $\mathcal{T}_0$ and $\mathcal{T}_1$.

- The turning operators $\mathcal{T}_0$ and $\mathcal{T}_1$ preserve the local mass

$$\int_V \mathcal{T}_0(f)\, dv = \int_V \mathcal{T}_1(S, f)\, dv = 0, \tag{6}$$

  for any $S \geq 0$.
- In addition, $\mathcal{T}_0$ conserves the population flux, that is,

$$\int_V \mathcal{T}_0(f)\, v\, dv = 0. \tag{7}$$

- For all $n \in [0, +\infty)$ and $u \in \mathbb{R}^d$, there exists a unique function $F_{n,u} \in L^1(V; (1 + |v|)dv)$ such that

$$\mathcal{T}_0(F_{n,u}) = 0\,, \quad \int_V F_{n,u}(v)\, dv = n, \quad \int_V F_{n,u}(v)\, v\, dv = n\, u. \tag{8}$$

The most commonly used assumption on the turning operators $\mathcal{T}_i$, $i = 0, 1$, is that they are both linear integral operators with respect to f and read

$$\mathcal{T}_i(S, f)(t, x, v) = \int_V \big(T_i(v, v') f(t, x, v') - T_i(v', v) f(t, x, v)\big)\, dv'. \tag{9}$$

Here the turning kernel $T_i(v, v')$ describes the reorientation of cells, i.e. the random velocity changes from v to v' and may depend on the chemo-attractant concentration and its derivatives. Notice that a straightforward consequence of the structure

(9) is that $\mathcal{T}_0$ and $\mathcal{T}_1$ fulfil (6). Moreover, the assumption (8) simply means that the kernel of $\mathcal{T}_0$ is $(d+1)$-dimensional. This is consistent with Remark 2.1 in Othmer & Hillen [11], where such a condition was expected for the hyperbolic or streaming character of the transport process to dominate. Usually, the assumption (7) on the conservation of the population flux by the operator $\mathcal{T}_0$ is not made, because classically, one prefers a diffusive scaling to recover PKS parabolic models. But here, it is useful in order to derive hyperbolic systems. We give later some examples where this additional conservation law can be derived.

2.2. Hydrodynamic limit

In this section, we explain why assumptions (6)–(8) lead to hyperbolic systems on a macroscopic scale. Let f be a solution to the kinetic equation (4) and set

$$n(t,x) = \int_V f(t,x,v)dv, \qquad n(t,x)\,u(t,x) = \int_V f(t,x,v)\,v dv. \tag{10}$$

We introduce f_1 such that

$$\varepsilon\, f_1(t,x,v) = f(t,x,v) - F_{n(t,x),u(t,x)}(v),$$

where the equilibrium distribution function $F_{n,u}$ is defined by (8). Then, the distribution f_1 satisfies the following properties

$$\int_V f_1(t,x,v)dv = \int_V f_1(t,x,v)\,v\,dv = 0.$$

We integrate (4) over $v \in V$ and use (10) and the conservation of mass (6) to obtain

$$\frac{\partial n}{\partial t} + \operatorname{div}(n\,u) = 0. \tag{11}$$

We next multiply (4) by v and integrate over V. Owing to the conservation of momentum (7) by the turning operator $\mathcal{T}_0$, we obtain

$$\frac{\partial (nu)}{\partial t} + \operatorname{div}\left(\int_V v\otimes v\, f(t,x,v)\,dv\right) = \int_V \mathcal{T}_1(S,f)\,v\,dv.$$

Replacing f by its expansion around the stationary state of $\mathcal{T}_0$

$$f(t,x,v) = F_{n(t,x),u(t,x)}(v) + \varepsilon f_1(t,x,v),$$

we are led to the following equation for the population flux $n\,u$

$$\frac{\partial (nu)}{\partial t} + \operatorname{div}\left(\int_V v\otimes v\, F_{n,u}(v)\,dv\right) = \int_V \mathcal{T}_1(S,F_{n,u})\,v dv + O(\varepsilon). \tag{12}$$

Next, we compute

$$\begin{aligned}\int_V v\otimes v\, F_{n,u}\,dv &= \int_V (v-u)\otimes(v-u)\,F_{n,u}\,dv + n\,u\otimes u,\\ &= P + n\,u\otimes u\end{aligned}$$

where the pressure tensor is given by

$$P(t,x) = \int_V (v - u(t,x)) \otimes (v - u(t,x))\, F_{n(t,x),u(t,x)}\, dv. \tag{13}$$

Moreover, since $\mathcal{T}_1$ also conserves local mass, (12) can be written as

$$\frac{\partial (nu)}{\partial t} + \mathrm{div}(n\, u \otimes u + P) = \int_V (v - u)\, \mathcal{T}_1(S, F_{n,u})\, dv + O(\varepsilon). \tag{14}$$

Then, to first order with respect to ε, we end up with the following hyperbolic system

$$\begin{cases} \dfrac{\partial n}{\partial t} + \mathrm{div}(n\, u) = 0, \\ \dfrac{\partial (nu)}{\partial t} + \mathrm{div}(n\, u \otimes u + P) = \displaystyle\int_V (v - u)\, \mathcal{T}_1(S, F_{n,u})\, dv, \end{cases} \tag{15}$$

the evolution of S being still given by the concentration equation (2).

We observe that the influence of the turning operator $\mathcal{T}_0$ on the macroscopic equations (15) only comes into play through the stationary state $F_{n,u}$ in the computation of the right-hand side of (15) and the pressure tensor P. The structure of the turning operator $\mathcal{T}_1$ determines the effect of the chemo-attractant.

The approach we have developed above is quite general and we now give more specific examples. In the literature, the turning operator is usually chosen to be linear with respect to f. We first consider this case, where the system (15) turns out to be also linear with respect to $(n, n\, u)$. In particular, a suitable choice of the turning operators $\mathcal{T}_0$ and $\mathcal{T}_1$ allows us to recover the Cattaneo system which has been extensively studied recently (see, e.g., [4, 13] and the references therein). We next derive nonlinear macroscopic models starting from a relaxation turning operator $\mathcal{T}_0$.

2.3. The Cattaneo system

We consider the case where the set of velocities is a sphere of radius s, $V = s\,\mathbb{S}^{d-1}$, with $s > 0$ and $\mathbb{S}^{d-1}$ the unit sphere of $\mathbb{R}^d$. Moreover, we assume the stationary state to be a linear combination of $1, v_1, \ldots, v_d$

$$F_{n,u}(v) = \frac{1}{\omega_0}\left(n + \frac{d}{s^2} n \sum_{i=1}^{d} v_i\, u_i\right),$$

where $\omega_0 = s^{d-1}|\mathbb{S}^{d-1}|$. We take $\mathcal{T}_0$ as a relaxation operator to $F_{n,u}$, that is,

$$\mathcal{T}_0(f) = \mu_0\,(F_{n,u} - f),$$

while $\mathcal{T}_1$ is given by

$$\mathcal{T}_1(f) = \mu_1\left(\frac{n}{\sigma_{d-1}} - f\right) - \frac{\mu_2 d}{s^2}\left(\frac{nu}{\sigma_{d-1}} - vf\right) \cdot \nabla S,$$

where n and u depend on f and are given by (10). Here, μ_i, $i = 0, 1, 2$, are real numbers and σ_{d-1} denotes the measure of $\mathbb{S}^{d-1}$. With the notations used in (9), these operators correspond to

$$T_0(v, v') = \frac{\mu_0}{\sigma_{d-1}} \left(1 + \frac{d}{s^2} v \cdot v'\right)$$

and

$$T_1(v, v') = \frac{\mu_1}{\sigma_{d-1}} - \frac{\mu_2 d}{\sigma_{d-1} s^2}\, v \cdot \nabla S.$$

Then, the pressure tensor $P = (P_{i,j})$ defined by (13) is

$$P_{i,j}(t, x) = \frac{s^2}{d} n - n\, u_i\, u_j$$

and

$$\int_V \mathcal{T}_1(S, F_{n,u})\, (v - u)\, dv = -\mu_1 n\, u + \mu_2 n\, \nabla S.$$

Then the model (15) becomes the following linear system

$$\begin{cases} \dfrac{\partial n}{\partial t} + \operatorname{div}(n\, u) = 0, \\ \dfrac{\partial (nu)}{\partial t} + \dfrac{s^2}{d} \nabla n = -\mu_1 n\, u + \mu_2 n\, \nabla S \end{cases} \tag{16}$$

which is called the Cattaneo model for chemosensitive movement with density control [4, 13]. One can actually include a more realistic dependence on S by choosing $\mu_2 = \mu_2(n, S)$.

This system has been already obtained by Hillen in [13] using a method of moments. The Chapman-Enskog expansion requires that the turning operator $\mathcal{T}_0$ preserves momentum (7) - a property which is of course fulfilled here - to get a system of equations for $(n, n\, u)$, whereas this assumption is not made in the moment closure method, where the number of unknowns is not directly related to the number of invariants of the turning operator $\mathcal{T}_0$. In addition, the Chapman-Enskog approach indicates that the solution to the hyperbolic system is an approximation of order ε of the density and population flux of the original transport equation (3), which is not clear for the method of moments. Indeed, recall that the latter is obtained from the system of equations for the moments of order zero and one of f with respect to v, which depends on the moments of f of order two, and is thus not closed. The closure is realized by approximating f by a function which maximizes an entropy [12]. Since there is no identified small parameter it does not seem to be obvious to show that the solution to the macroscopic system is an approximation of the moments of the solution f to (3).

Observe that the Cattaneo model (16) is also linear with respect to $(n, n\, u)$. Other choices of $\mathcal{T}_1$, depending on S, are proposed and investigated numerically in [4]. In particular, assuming a nonlinear dependence of μ_2 in (16) on n, numerical

experiments are performed in [4] to observe pattern formation and seem to give good results which agree well with experiments.

However, one drawback of this macroscopic model is that the density $n(t, x)$ need not be nonnegative. Indeed, it satisfies a linear wave equation with a source term and the positivity is not preserved during the evolution in general.

2.4. Nonlinear relaxation models

As already mentioned, the geometrical structure of the turning operator $\mathcal{T}_0$ does not play a major role in the derivation of macroscopic models in our approach, since it only appears through the stationary states in (8). For this reason, we here only consider relaxation models associated with a given stationary solution F. For simplicity we choose $V = \mathbb{R}^d$ and consider a nonnegative function $F \in L^1(V, (1 + |v|)dv)$, a positive function $\vartheta : \mathbb{R} \longrightarrow (0, +\infty)$ and $\lambda > 0$, such that

$$\int_V F(v)\, dv = 1, \quad \int_V v\, F(v)\, dv = 0.$$

and

$$\mathcal{T}_0(f)(v) = \lambda \left(\frac{n}{\vartheta^{d/2}(n)} F\left(\frac{v-u}{\vartheta^{1/2}(n)} \right) - f(v) \right).$$

Here again, n and u depend on f and are given by (10). Thanks to the structure of $\mathcal{T}_0$ and the properties of F, $\mathcal{T}_0$ clearly enjoys (6), (7) and (8). Presently, this turning operator may lack a biological interpretation, but as we said before, macroscopic quantities do not depend on the specific structure of the turning operator $\mathcal{T}_0$. Nevertheless, this operator might be seen as a coarse model for local interactions between the cells, which can be observed in some recent experiments with human endothelial cells on matrigel [24]. Also, it has the advantage of compatibility with nonnegative densities. These are the reasons why such relaxation operators are widely used in physics and their mathematical properties well studied [29]. On the other hand, the structure of the turning operator $\mathcal{T}_1$ is much more important because the dynamics is mainly driven by the chemoattractant and we present different models below.

The computation performed in §2.2 allows us to derive the pressure tensor, which only depends on the stationary state of $\mathcal{T}_0$ and reads

$$P = \frac{n}{\vartheta^{d/2}(n)} \int_V (v-u) \otimes (v-u) F\left(\frac{v-u}{\vartheta^{1/2}(n)} \right) dv = n\vartheta(n)\, p,$$

with the constant matrix p given by

$$p = \int_V v \otimes v F(v) dv.$$

2.4.1. Scattering-type turning operator $\mathcal{T}_1$
We consider here that $\mathcal{T}_1 = \mathcal{T}_1(S, f)$ is given by

$$\mathcal{T}_1(S, f) = \int_V K_1(v, v', S) \cdot \nabla S \, f(v') \, dv' - \int_V K_1(v', v, S) \cdot \nabla S \, dv' \, f(v).$$

Obviously, $\mathcal{T}_1$ satisfies (6) and we easily check that

$$\begin{aligned}
&\int_V (v-u) \, \mathcal{T}_1(S, F_{n,u}) \, dv \\
&\quad = \frac{n}{\vartheta^{d/2}(n)} \int_{V\times V} v \, K_1(v, v', S) \cdot \nabla S \, F\left(\frac{v'-u}{\vartheta^{1/2}(n)}\right) dv dv' \\
&\qquad - \frac{n}{\vartheta^{d/2}(n)} \int_{V\times V} K_1(v', v, S) \cdot \nabla S \, F\left(\frac{v-u}{\vartheta^{1/2}(n)}\right) dv' \, dv, \\
&\quad = n \, \vartheta^{(d+1)/2}(n) \; \chi \, (n, u, S) \, \nabla S,
\end{aligned}$$

where the matrix χ is given by

$$\chi(n, u, S) = \int_{V\times V} (v - v') \otimes K_1(u + \vartheta^{1/2} v, u + \vartheta^{1/2} v', S) F(v') \, dv' \, dv.$$

We then obtain the following model for the cell movements

$$\begin{cases} \dfrac{\partial n}{\partial t} + \operatorname{div}(n \, u) = 0, \\ \dfrac{\partial (nu)}{\partial t} + \operatorname{div}(n \, u \otimes u + n \vartheta(n) p) = n \, \vartheta^{(d+1)/2}(n) \; \chi(n, u, S) \nabla S, \end{cases} \tag{17}$$

coupled with the concentration equation (2) for S.

2.4.2. Nonlinear turning operator $\mathcal{T}_1$
More generally, the turning operator $\mathcal{T}_1$ may also depend nonlinearly on f. For instance, when only macroscopic quantities computed from the distribution function f are taken into account, a possible choice is

$$\mathcal{T}_1(S, f) = \int_V K_1(v - u, v' - u, n, S) \cdot \nabla S f(v') dv'.$$

Then,

$$\begin{aligned}
&\int_V (v-u) \mathcal{T}_1(S, F_{n,u}) dv \\
&\quad = \frac{n}{\vartheta^{d/2}} \int_{V\times V} (v-u) \otimes K_1(v-u, v'-u, n, S) F\left(\frac{v-u}{\vartheta^{d/2}}\right) dv dv' \, \nabla S, \\
&\quad = n \, \chi(n, S) \, \nabla S,
\end{aligned}$$

where the matrix χ is given by

$$\chi(n, S) = \vartheta^{(d+1)/2}(n) \int_{V\times V} w \otimes K_1(\vartheta(n)^{1/2} w, \vartheta(n)^{1/2} w', n, S) F(w') dw dw'.$$

We finally show that the model for blood vessels formation introduced in [31,8] can be obtained from (4) by the approach we have developed, with a turning operator $\mathcal{T}_1$ depending nonlinearly on f. More precisely, we assume further that

$$K_1(v, v', n, S) = a(n)\, l_1(v) v,$$

with

$$\int_V l_1(v)\, dv = 1, \quad \int_V v\, l_1(v)\, dv = 0, \quad \int_V v \otimes v\, l_1(v) dv = Id.$$

We then obtain

$$\int_V (v - u)\mathcal{T}_1(S, F_{n,u}) dv = a(n)\, n\, \vartheta^{(d+1)/2}(n)\, \nabla S.$$

Taking $a(n) = \vartheta^{-(d+1)/2}(n)$, we end up with the following system proposed by Gamba *et al.* in [31,8]

$$\begin{cases} \dfrac{\partial n}{\partial t} + \operatorname{div}(n\, u) = 0, \\ \dfrac{\partial (nu)}{\partial t} + \operatorname{div}(n\, u \otimes u + n\vartheta(n)\, p) = n \nabla S, \end{cases} \tag{18}$$

still coupled with the concentration equation (2) for S. The model considered in [31,8] is actually (18) with $p = Id$ coupled to (2) and is used to describe vasculogenesis (early formation of blood vessels). This model has also been used to describe the emergence of network-like patterns in the large-scale distribution of masses of the Universe [34].

At this stage we may discuss more precisely the differences between hyperbolic systems as (18)–(2) and parabolic systems as PKS model (1)–(2). Both of them exhibit singular pattern formation, and in particular blow-up patterns. There is however a striking difference between the transient states before the blow-up occurs. Indeed, for the PKS parabolic model (1)–(2), the density n of cells concentrates in the neighbourhood of isolated points, these concentration regions becoming more and more narrow and ultimately leading to finite time pointwise blow-up. We refer to [10,21,33] for mathematical proofs for spherically symmetric solutions in a ball, the blow-up point being the center of the ball (and these are the only possible singularities). In the nonsymmetric case blow-up results are established in [14, 15,30], the blow-up points being located on the boundary. Numerical evidence of this fact may be found in [23], see also [7], remark 4.5. This pointwise blow-up is compatible with well-established experiments for *Dictyostelium Discoïdeum* or *Escherichia Coli*. On the other hand, finite time blow-up was also proved in [22] for spherically symmetric solutions to the hyperbolic system (18). But it is more expected that shock-type structures appear before blow-up, which could explain that the density concentrates in the vicinity of the edges of a network. These are indeed recovered in the numerical simulations below and seem to be compatible with the experiments on endothelial cells.

Remark 1. System (18) can be also derived as an hydrodynamic limit of the Vlasov-Fokker-Planck equation, which appears in the study of the mass distribution in the Universe and reads

$$\frac{\partial f}{\partial t} + v \cdot \nabla_x f + \nabla S \cdot \nabla_v f = \frac{1}{\varepsilon} \mathcal{T}_0(f) \tag{19}$$

where $\mathcal{T}_0$ is the nonlinear Fokker-Planck operator

$$\mathcal{T}_0(f) = \mathrm{div}_v \left((v-u) f + \vartheta(n) \nabla_v f \right),$$

the concentration S is given by (2) and $(n, n\,u)$ represents the density and the population flux computed from f given by (10). The stationary state of the Fokker-Planck operator is the Maxwellian

$$\mathcal{M}_{n,u}(v) = \frac{n}{(2\,\pi\,\vartheta(n))^{d/2}} \exp\left(-\frac{|v-u|^2}{\vartheta(n)} \right),$$

and the pressure tensor reads

$$P = \int_{\mathbb{R}^d} (v-u) \otimes (v-u)\, \mathcal{M}_{n,u}(v)\, dv = n\,\vartheta(n)\, Id.$$

Performing a similar Chapman-Enskog expansion on (19), we recover (18). Moreover, a diffusive limit of the Vlasov-Fokker-Planck model (19) with $u = 0$ allows us to get the parabolic PKS model (1)–(2) [25]. Thus, at the kinetic level the Vlasov-Fokker-Planck model may also be an interesting approach to the study of cell movements.

We conclude this section by some remarks on the connection between the hyperbolic chemotaxis model (18)–(2) and the parabolic chemotaxis model (1)–(2). We first notice that, when $p = Id$, the stationary solutions to (18) with a zero population flux ($n\,u = 0$) are the same as those of the PKS model. Indeed, such stationary solutions satisfy

$$n \nabla S - \nabla(n \vartheta(n)) = 0,$$

which is the equation satisfied by stationary solutions to the diffusive model for chemotaxis [26,27]. Finally, a further rescaling in time and space of the hyperbolic model formally leads to the parabolic system (1)–(2) - see [20].

3. Numerical simulations

We now present some numerical simulations on the nonlinear hyperbolic system (18), (2) and first briefly describe the numerical scheme in a two-dimensional setting. We refer to [6] for a more precise description of high order methods and for more numerical experiments showing the accuracy and robustness of the scheme to approximate non-smooth solutions to nonlinear hyperbolic systems as (18), (2).

We write (18) in the following form

$$\frac{\partial U}{\partial t} + \nabla_x \cdot F(U) = R(U), \tag{20}$$

where

$$U = \begin{pmatrix} n \\ n\,u \end{pmatrix}, \quad F(U) = \begin{pmatrix} n\,u_1 & n\,u_2 \\ n\,u_1^2 + n\,\vartheta(n) & n\,u_1\,u_2 \\ n\,u_1\,u_2 & n\,u_2^2 + n\vartheta(n) \end{pmatrix},$$

with $u = (u_1, u_2)$ and the source term is

$$R(U) = \begin{pmatrix} 0 \\ n\,\nabla_x S \end{pmatrix}.$$

We fix a time step Δt and set $t^k = k\,\Delta t$. The method is based on a time splitting scheme between the conservative part and the source term, that is, the approximation U^{k+1} of $U(t^{k+1})$ is computed from the approximation U^k of $U(t^k)$ in two steps:

$$U^{k+1/2} = U^k - \Delta t \nabla_x \cdot F(U^k), \tag{21}$$

and

$$U^{k+1} = U^{k+1/2} + \Delta t\, R(U^{k+1/2}). \tag{22}$$

We next turn to the space discretization and consider grid points $(x_i)_{i\in\mathbb{N}}$ in the box $(0, L)^2$. We approximate the solution $U^k(x)$ by discrete values U_i^k. A finite volume method is used for solving (21). On the one hand, the discretization of the conservative part is performed by integrating (21) on the square C_i centered at x_i. The approximation $U_i^{k+1/2}$ is given by

$$U_i^{k+1/2} = U_i^k + \frac{\Delta t}{\Delta x^2}(F_{i+1/2} - F_{i-1/2}).$$

Here, the flux $F_{i+1/2}$ is approximated by the Lax-Friedrichs flux [9,18]

$$F(U_r, U_l) = \frac{1}{2}(F(U_r) + F(U_l)) + \frac{\alpha}{2}(U_l - U_r),$$

where α is an upper bound of the Jacobian $|\nabla_x F|$, and U_r (resp. U_l) is a high order reconstruction of U^k in C_i (resp. C_{i+1}). On the other hand the diffusion equation (2) is approximated by a classical second order finite difference scheme [18].

3.1. Influence of the population flux

We first present a simple numerical test to figure out the influence of the new variable $n\,u$ (population flux) on the dynamics. For that purpose, we perform a comparison between the PKS model (1)

$$\frac{\partial n}{\partial t} - \operatorname{div}(\nabla n - n\nabla S) = 0 \tag{23}$$

and the nonlinear hyperbolic model (18) with the choice $\vartheta(n) = 1$ and $p = Id$

$$\frac{\partial n}{\partial t} + \operatorname{div}(n\,u) = 0, \tag{24}$$

$$\frac{\partial (nu)}{\partial t} + \operatorname{div}(n\,u \otimes u + n\,Id) = n \nabla S. \tag{25}$$

In both cases, the evolution of S is still given by (2) with the choice $g(n, S) = n$

$$\frac{\partial S}{\partial t} - D_S\,\Delta S = n. \tag{26}$$

For the numerical simulations, we take $D_S = 0.001$ and the initial datum $S(0) = 0$. For the density and population flux, we consider an initial datum, which is at rest $u(0) = 0$ and a distribution of cells with high density in two localized regions

$$n(0, x, y) = \frac{n_0}{2\,\pi\,\sigma^2}\left(e^{-\left((x-x_0)^2+(y-y_0)^2\right)/2\,\sigma^2} + e^{-\left((x+x_0)^2+(y+y_0)^2\right)/2\,\sigma^2}\right), \tag{27}$$

where $n_0 = 1/4$, $(x_0, y_0) = (3\,\sigma, 3\,\sigma)$ and $\sigma = 3.\,10^{-2}$.

In Figs 2 and 3, we present the numerical solution for the parabolic model (23) and (26) and the hyperbolic model (24), (25) and (26). Clearly, the transient behaviour of the two models differs due to the non-vanishing variation of the population flux $(n\,u)$. In the hyperbolic system (Fig. 3), we also observe the appearance of a third bump between the two initial high density regions of n, where the population flux is the largest. During time evolution we observe the elongation of the third bump which can be interpreted as a first step of the formation of an edge of density

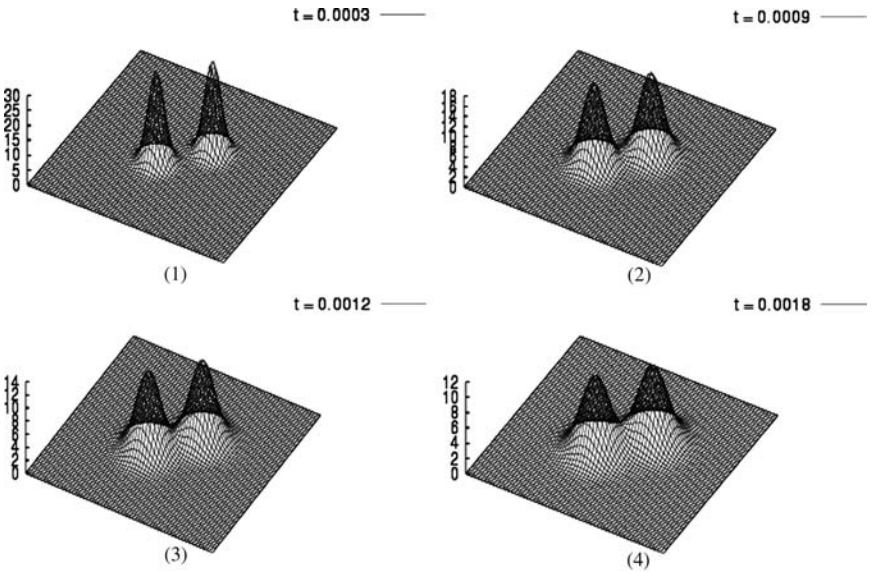

Fig. 2. Chemosensitive movement: *evolution of the cell density $n(t, x)$ obtained from the parabolic PKS model.*

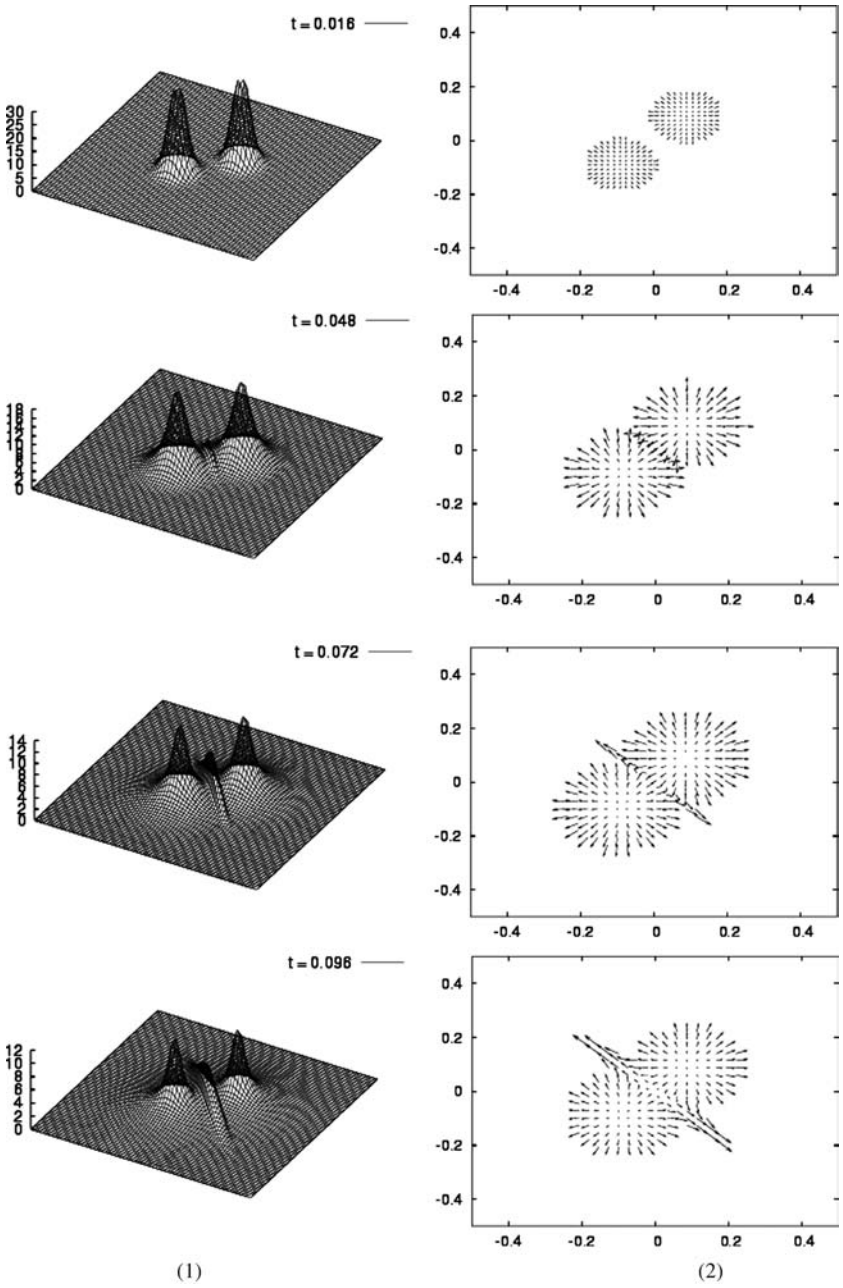

Fig. 3. Chemosensitive movement: *evolution of (1) the cell density $n(t, x)$ and (2) the velocity field $u(t, x)$ obtained from the nonlinear hyperbolic model.*

concentration. Also, we note that the final maximal value of the density n is the same in both simulations, but the final time is larger for the hyperbolic model than for the parabolic one. This is expected because of the finite speed of propagation property enjoyed by the former.

3.2. Formation of networks

As in [31,8], we perform numerical simulations of the hyperbolic model (18), (2) on a square box of length $L = 0.2\ cm$ with periodic boundary conditions, using a finite difference method. We set

$$g(S, n) = \alpha\, n - \frac{1}{\tau}\, S$$

in (2), where α represents the rate of release and τ is the characteristic degradation time of soluble mediators. Here, we take $\alpha = 1$, $\tau = 3600\ sec.$ and the diffusion rate in (2) is $D_S = 10^{-7}$, which correspond to the choice made in [31,8]. We also choose the pressure to be

$$\vartheta(n) = (\sigma^2\, n)^3,$$

where σ is the mean cell radius, which is of order 30 $\mu\, m$.

The initial datum $n(0)$ is chosen by throwing randomly cells inside the box, with zero population flux $(n\, u)(0) = 0$ and zero concentration $S(0) = 0$ initially. More precisely, for $(x, y) \in (0, L)^2$, we choose

$$n(0, x, y) = \frac{1}{(2\,\pi\,\sigma)^2} \sum_{i=1}^{N} \exp\left(-\left((x - x_i)^2 + (y - y_i)^2\right)/2\,\sigma^2\right),$$

where $(x_i, y_i)_{1 \le i \le N}$ are uniformly distributed random points in the box $(0, L)^2$, each Gaussian bump of width σ representing a single cell. Thus N denotes the total number of cells.

We present different numerical simulations when the initial total cell density N varies. The simulation is stopped when either a stationary state is reached or the network is formed.

In Fig. 4, the cell density is only 50 $cells/mm^2$. Cells become closer and closer, but the total density is not high enough to initiate a network. In Fig. 5 and 6, the density is taken as 100 $cells/mm^2$ and 400 $cells/mm^2$, respectively. We then observe the formation of high density regions which are joined by chords. These results reproduce well experiments (see Fig. 1 or [31,8]).

4. Discussion

In this paper we have developed a unified approach relying on the Chapman-Enskog expansion to understand the link between kinetic models and hyperbolic systems of chemotaxis. Using an appropriate scaling of the kinetic transport equations we derive macroscopic models for the cell density and population flux. In contrast to the moment method, our approach guarantees (at least formally) that the solution to the macroscopic model (15) is indeed an approximation of order one (with respect

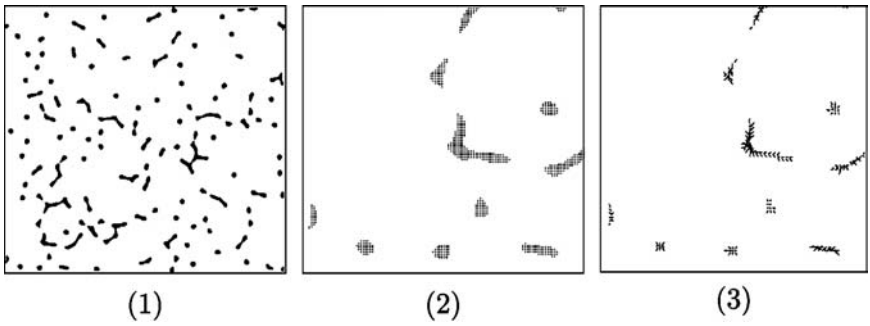

Fig. 4. Formation of network:*(1) density and zoom on the left-bottom corner of (2) the density and (3) velocity field obtained with* 50 $cells/mm^2$.

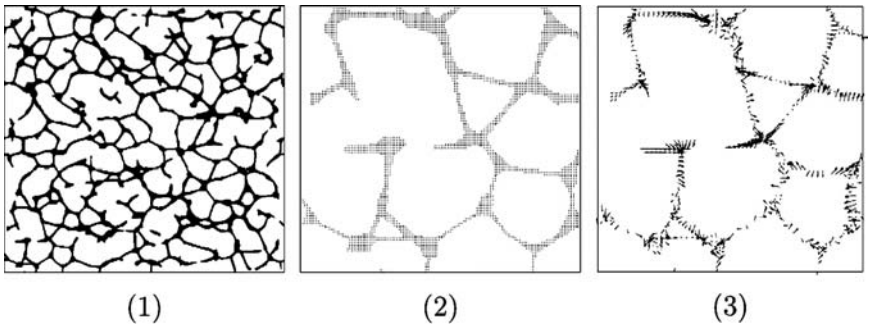

Fig. 5. Formation of network:*(1) density and zoom on the left-bottom corner of (2) the density and (3) velocity field obtained with* 100 $cells/mm^2$.

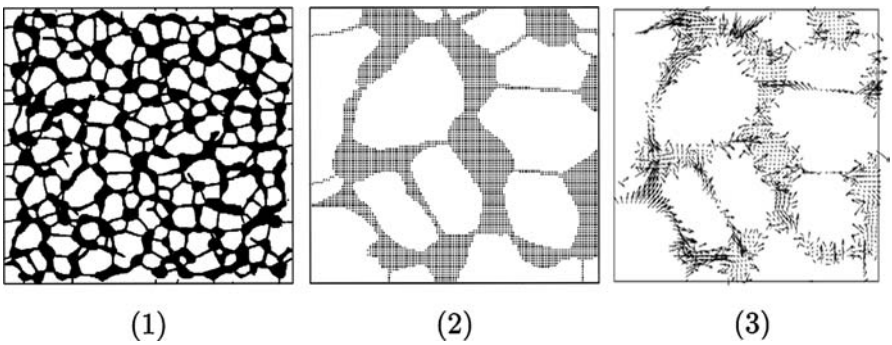

Fig. 6. Formation of network: *(1) density and zoom on the left-bottom corner of (2) the density and (3) velocity field obtained with* 400 $cells/mm^2$.

to the rescaling parameter ε) to the cell density and population flux of the solution to the kinetic equation (3). Furthermore, it provides explicitly formulae for the flux $n\,u \otimes u + P$ associated to the population flux $n\,u$ and the chemotactic sensitivity χ in terms of the turning operator $\mathcal{T}$, which is not the case in the previous empirical derivations [31].

From a mathematical viewpoint, the rigorous convergence of the nonlinear kinetic equation to the hyperbolic system is an interesting issue, but this kind of problem is currently one of the main open questions in kinetic theory [29]. A first step in this direction would be to prove the existence of a solution to the hyperbolic system which is beyond the scope of this paper.

We have also developed a numerical scheme to solve hyperbolic models for chemosensitive movement. A high order approximation has been subsequently implemented in [6], where further numerical simulations have been performed. Let us mention here that the difficulty encountered in a convergence proof for one of these schemes is similar to the one mentioned above for an existence result.

In summary, chemosensitive movement models are the starting point to perform computer simulations of biological processes, which can be compared with experiments [31]. Based on these mathematical derivations at the kinetic scale and numerical simulations, this paper gives a hint that network formations for human endothelial cells on matrigel could be also due to local interactions and not only to long range interactions. More precisely, hyperbolic models seem to represent well the phenomena and can be derived from a local interaction kernel at the kinetic level.

Acknowledgements. The authors thank M. Mirshahi (INSERM E355 - Faculté de Médecine de Paris VI) for fruitful discussions and providing experimental data. Helpful discussions on numerical and modeling issues with A. Gamba and M. Lemou are gratefully acknowledged. This work was also partially supported by the European network HYKE, funded by the EC as contract HPRN-CT-2002-00282.

References

[1] Alt, W.: Biased random walk models for chemotaxis and related diffusion approximations. J. Math. Biol. **9**, 147–177 (1980)

[2] Chalub, F.A.C.C., Markovich, P., Perthame, B., Schmeiser, C.: Kinetic models for chemotaxis and their drift-diffusion limits. To appear in Monatsh. Math.

[3] Chaplain, M.A.J.: A vascular growth, angiogenesis and vascular growth in solid tumors: the mathematical modelling of the stages of tumor development. Math. Comput. Modelling **23**, 47–87 (1996)

[4] Dolak, Y., Hillen, T.: Cattaneo models for chemotaxis, numerical solution and pattern formation. J. Math. Biol. **46**, 461–478 (2003)

[5] Dolak, Y., Schmeiser, C.: Kinetic models for chemotaxis: Hydrodynamic limits and the back-of-the-wave problem. ANUM preprint

[6] Filbet, F., Shu, C.-W.: Approximation of Hyperbolic Models for Chemosensitive Movement. MAPMO preprint

[7] Gajewski, H., Zacharias, K.: Global behavior of a reaction diffusion system modelling chemotaxis. Math. Nachr. **195**, 77–114 (1998)

[8] Gamba, A., Ambrosi, D., Coniglio, A., de Candia, A., Di Talia, S., Giraudo, E., Serini, G., Preziosi, L., Bussolino, F.: Percolation, morphogenesis, and Burgers dynamics in blood vessels formation. Phys. Rev. Lett. **90**, 118101 (2003)

[9] Godlewski, E., Raviart, P.-A.: Numerical approximation of hyperbolic systems of conservation laws. Appl. Math. Sci. **118**, Springer, New York, 1996

[10] Herrero, M.A., Medina, E., Velázquez, J.J.L.: Finite-time aggregation into a single point in a reaction-diffusion system. Nonlinearity **10**, 1739–1754 (1997)

[11] Hillen, T., Othmer, H.G.: The diffusion limit of transport equations derived from velocity jump processes. SIAM J. Appl. Math. **61**, 751–775 (2000)

[12] Hillen, T.: Transport equations and chemosensitive movement. Habilitation Thesis, University of Tübingen, 2001

[13] Hillen, T.: Hyperbolic models for chemosensitive movement. Math. Models Methods Appl. Sci. **12**, 1007–1034 (2002)

[14] Horstmann, D.: From 1970 until now: The Keller-Segel model in chemotaxis and its consequences I. Jahresberichte der DMV, **105**, 103–165 (2003)

[15] Horstmann, D.: From 1970 until now: The Keller-Segel model in chemotaxis and its consequences II. Jahresberichte der DMV, **106**, 51–69 (2004)

[16] Hwang, H.J., Kang, K., Stevens, A.: Global solutions of nonlinear transport equations for chemosensitive movement. To appear in SIAM J. Math. Anal.

[17] Keller, E.F., Segel, L.A.: Traveling band of chemotactic bacteria: A theoretical analysis. J. Theor. Biol. **30**, 235–248 (1971)

[18] LeVeque, R.: Numerical methods for conservation laws. Birkhäuser, Basel, 1992

[19] Levine, H.A., Nilsen-Hamilton, M., Sleeman, B.D.: Mathematical modelling of the onset of capillary formation initiating angiogenesis. J. Math. Biol. **42**, 195–238 (2001)

[20] Liu, T.P.: Hyperbolic conservation laws with relaxation. Comm. Math. Phys. **108**, 153–175 (1987)

[21] Nagai, T.: Blow-up of radially symmetric solutions to a chemotaxis system. Adv. Math. Appl. Sci. **5**, 581–601 (1995)

[22] Makino, T., Perthame, B.: Sur les solutions à symétrie sphérique de l'équation d'Euler-Poisson pour l'évolution d'étoiles gazeuses. Japan J. Appl. Math. **7**, 165–170 (1990)

[23] Marrocco, A.: 2D simulation of chemotaxis bacteria aggregation. ESAIM:M2AN, **37** (4), 617–630 (2003)

[24] Mirshahi, M.: Personnal communication

[25] Nieto, J., Poupaud, F., Soler, J.: High-field limit for the Vlasov-Poisson-Fokker-Planck system. Arch. Rational Mech. Anal. **158**, 29–59 (2001)

[26] Othmer, H.G., Hillen, T.: The diffusion limit of transport equations II: chemotaxis equations. SIAM J. Appl. Math. **62**, 1222–1250 (2002)

[27] Othmer, H.G., Dunbar, S.R., Alt, W.: Models of dispersal in biological systems. J. Math. Biol. **26**, 263–298 (1988)

[28] Patlak, C.S.: Random walk with persistence and external bias. Bull. Math. Biol. Biophys. **15**, 311–338 (1953)

[29] Perthame, B.: Kinetic formulation of conservation laws. Oxford Univ. Press, 2002

[30] Senba, T., Suzuki, T.: Chemotactic collapse in parabolic-elliptic systems of mathematical biology. Adv. Diff. Eqns. **6**, 21–50 (2001)
[31] Serini, G., Ambrosi, D., Giraudo, E., Gamba, A., Preziosi, L., Bussolino, F.: Modeling the early stages of vascular network assembly. The EMBO J. **22**, 1771–1779 (2003)
[32] Stevens, A.: Derivation of chemotaxis-equations as limit dynamics of moderately interacting stochastic many particle systems. SIAM J. Appl. Math. **61**, 183–212 (2000)
[33] Velázquez, J.J.L.: Stability of some mechanisms of chemotactic aggregation. SIAM J. Appl. Math. **62**, 1581–1633 (2002)
[34] Zeldovich, Ya.B.: Gravitational instability : an approximate theory for large density perturbations. Astron. Astrophys. **5**, 84 (1970)